

A Novel Two-Layer Passive Optical Interconnection Network for On-Chip Communication

Ke Chen, Huaxi Gu, Yintang Yang, and Dongrui Fan, *Member, IEEE*

Abstract—Passive optical interconnection network (OIN) plays a key role in optical Network-on-Chip (ONoC) architecture. Existing passive OINs based on wavelength division multiplexing (WDM) are popularly employed. However, the scalability of these passive OINs is limited by the number of wavelengths and large insertion loss induced by the waveguide crossings. In this paper, we propose a novel Passive OIN based on two-layer architecture, POINT, for ONoC architecture. POINT leverages space division multiplexing (SDM) to assist WDM in eliminating blocking. The inter-layer communication in POINT relies on the inter-layer coupler, which contributes to reduce crossing losses. POINT features a modular and scalable design, in which the proposed SDM-based cell (SBC) is used as the basic building block to construct POINT with efficient wavelength assignment. Furthermore, SBCs of different sizes provide different options for constructing POINT. Comparisons with existing passive OINs confirm that POINT can provide an optimal choice with the balance between the number of wavelengths, area overhead, and insertion loss for the same size.

Index Terms—Inter-layer coupler, network-on-chip, optical interconnect, passive network.

I. INTRODUCTION

OPTICAL network-on-chip (ONoC) has been proposed as a promising solution to interconnect a large number of IP (Intellectual Property) cores in the multi-processor system-on-chip (MPSoC) [1]–[7]. The ONoC architecture consists of three main sets of building-blocks: the transmitting-path block (Tx-Path), the optical interconnection network (OIN), and the receiving-path block (Rx-Path). System-on-chip IP cores are connected to ONoC through network interfaces (NIs), as shown in Fig. 1 [8]. The heart of the ONoC is the on-chip OIN, which is responsible for the propagation of optical signals from the source to the destination.

Manuscript received September 15, 2013; revised December 9, 2013 and February 1, 2014; accepted March 3, 2014. Date of publication March 10, 2014; date of current version April 10, 2014. This work was supported by the National Science Foundation of China under Grants 61070046, 61334003, and 61173007, the National Grand Fundamental Research 973 Program of China under Grant 2011CB302501, the Fundamental Research Funds for the Central Universities under Grant K5051301003, the 111 Project under Grant B08038, the State Key Laboratory of Computer Architecture under Grant CARCH201306.

K. Chen and H. Gu are with the State Key Laboratory of Integrated Service Networks, Xidian University, Xi’an 710071, China (e-mail: takechen01@126.com; hxgu@xidian.edu.cn).

Y. Yang is with the Institute of Microelectronics, Xidian University, Xi’an 710071, China (e-mail: ytyang@xidian.edu.cn).

D. Fan is with the State Key Laboratory of Computer Architecture, Institute of Computing Technology, Beijing 100190, China (e-mail: fandr@ict.ac.cn).

Color versions of one or more of the figures in this paper are available online at <http://ieeexplore.ieee.org>.

Digital Object Identifier 10.1109/JLT.2014.2311119

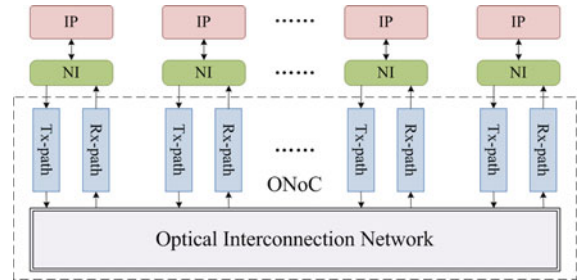


Fig. 1. Optical network-on-chip architecture.

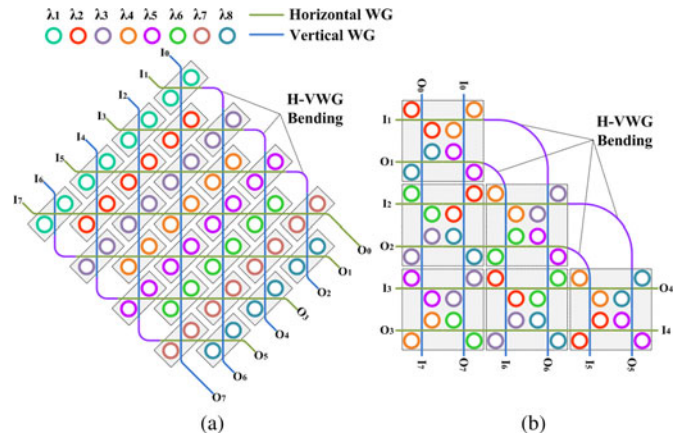


Fig. 2. Two passive OINs. (a) 8×8 λ -router. (b) 8×8 GWOR. (The symbol I (O) represents the input (output) port connected with the transmitting-path (receiving-path) block, the i th (j th) input (output) port is denoted as I_i (O_j .)

Several OINs have been proposed, which employ the microring resonator (MR) as the basic switching element. These OINs can be classified as either active OINs or passive OINs. Active OINs employ active-type MRs [9]–[11] where the resonant wavelength is controlled by voltage or thermal effect. Passive OINs utilize passive-type MRs [12], [13] where the resonant wavelength is determined by the material and geometrical dimensions. Active OINs can provide higher bandwidth, requiring extra control circuits which have adverse impacts on power consumption, while passive OINs own the advantage of saving energy owing to the wavelength routing instead of the extra control circuits.

Some passive OINs have been proposed. As the first passive OIN, the λ -router [12] consists of N stages of 2×2 optical switches. Fig. 2(a) presents an example of 8×8 λ -router architecture. Each stage is composed of optical switches characterized by the same resonant wavelength and linked through waveguides. An $N \times N$ λ -router needs N wavelengths totally. Another absorbing passive OIN is the GWOR (Generic

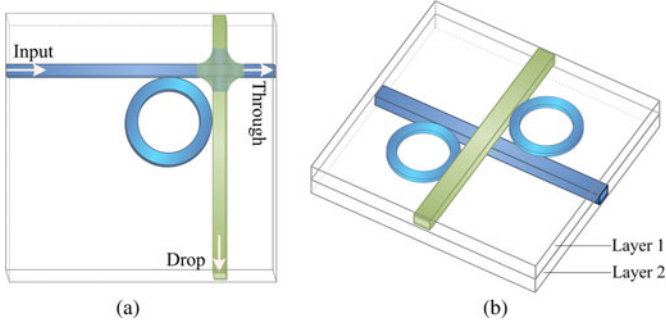


Fig. 3. (a) Basic operation of MR, optical signals with the resonant wavelength are filtered to drop port while all other signals continue to through port. (b) Three-dimensional schematic representation of the inter-layer coupler.

Wavelength-routed Optical Router) proposed in [13]. GWOR improves the scalability with fewer wavelengths and MRs compared with λ -router. As shown in Fig. 2(b), 4×4 GWOR is used as the primitive building block to build GWORs of larger sizes. In an $N \times N$ GWOR, $N - 2$ types of MRs and $N - 1$ wavelengths are needed.

By using wavelength division multiplexing (WDM) technique, multicasting/broadcasting and many-to-one communication can be supported by both λ -router and GWOR. Any input (I) can communicate with many outputs (O) simultaneously with multiple wavelengths. Also, signals from multiple inputs can be multiplexed to a single output without arbitration. N^2 ($(N - 1)^2$) simultaneous communications between N inputs and N outputs are supported in the λ -router (GWOR) without conflict. However, the scalability of both λ -router and GWOR is limited by the amount of wavelengths, which is currently technologically limited [14]–[16]. Therefore, we use multiple waveguides to relieve the pressure on multiple wavelengths and provide sufficient number of communication channels.

Insertion loss is a critical figure of merit for a passive OIN, which determines the feasibility and scalability, as well as the power consumption for generating and detecting the optical signal. For both λ -router and GWOR, as they scale to support more IP cores, more and more waveguide crossings are introduced in the architectures, incurring higher insertion losses. To solve this problem, we consider employing an appealing device named inter-layer coupler, which is used for 3-D optical interconnect [17], [18], as shown in Fig. 3(b). It has two functions: i) implementing the basic function of an MR [see Fig. 3(a)]; ii) coupling optical signal from one silicon layer to another. There is no waveguide crossing, where the horizontal waveguides (HWGs) and vertical waveguides (VWGs) are stacked vertically, thus avoiding the crossing losses. However, it is hard to apply the inter-layer coupler to λ -router and GWOR, because of the existence of the H-VWG bendings. Such bendings connects HWGs with VWGs and require all the waveguides to stay in the plane, which can be seen from Fig. 2. Therefore, we realize the architectural innovation without H-VWG bendings to leverage the advantages of inter-layer couplers.

In this paper, we propose a novel passive OIN based on two-layer architecture (POINT), which is a symmetrical and scalable architecture that combines WDM, space division

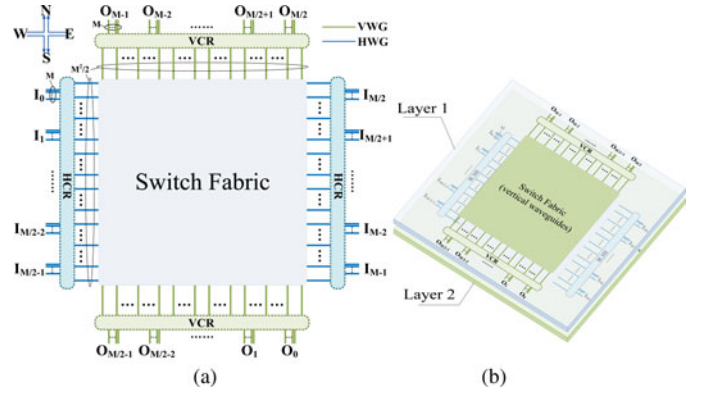


Fig. 4. The $M \times M$ SDM-based cell. (a) 2-D layout. (b) 3-D layout (where E , W , S , and N indicate East, West, South, and North, respectively).

multiplexing (SDM), and inter-layer couplers to develop a non-blocking passive OIN. We first utilize SDM to introduce the $M \times M$ SBC (SDM-based Cell) architecture created by re-using only one wavelength on different communication channels and then utilize WDM to construct $N \times N$ POINT using the proposed SBC as the basic building block with efficient wavelength assignment. SBCs of different sizes offer different options for constructing POINT of different sizes. Comparisons with λ -router and GWOR show that POINT can provide an optimal choice with the balance between the number of wavelengths, area overhead and insertion loss for the same size.

The remainder of this paper is organized as follows. Section II presents the architecture of $M \times M$ SDM-based cell and Section III shows how to construct $N \times N$ POINT using the proposed $M \times M$ SBC. In section V, we compare the four kinds of representative POINT with existing passive OINs in terms of the number of wavelengths, area overhead, and the insertion loss. Finally, section VI concludes the paper.

II. ARCHITECTURE OF $M \times M$ SDM-BASED CELL

In this section, the $M \times M$ (where $M = 1$ or $M = 2m$ and $m > 0$) SDM-based cell is first introduced as the basic building block to build $N \times N$ (where $N = 2n$ and $N \geq M$) POINT. As shown in Fig. 4, the core element of an $M \times M$ (where $M = 2m$ and $m > 0$) SBC is the central switch fabric, which is responsible for transmitting optical signals from their input ports to their output ports. In the switch fabric, $M^2/2$ horizontal (vertical) waveguides are sequentially numbered $0-M^2/2-1$ from north (east) to south (west). These M^2 waveguides together form a cross-grid architecture. $M/2$ input (output) ports are located at the west (south) side of the switch fabric and are sequentially numbered $0-M/2-1$ from north (east) to south (west), and the other $M/2$ ones are located at the east (north) side and are sequentially numbered $M/2-M-1$ from north (east) to south (west). Each input (output) port contain M horizontal (vertical) waveguides, which are sequentially numbered $0-M-1$ from north (east) to south (west).

From the introduction above, optical signals from the input ports are always injected into the horizontal waveguides and ejected from the vertical ones. That is, the signal has to traverse

TABLE I
FOUR TURNS FOR ALL THE COMMUNICATIONS

	$O_0 \sim O_{M/2-1}$	$O_{M/2} \sim O_{M-1}$
$I_0 \sim I_{M/2-1}$	WS turn	WN turn
$I_{M/2} \sim I_{M-1}$	ES turn	EN turn

a 90° turn before arriving at the destination. Table I shows there are four types of turns, namely WN, WS, EN, and ES turn.

Fig. 4(b) shows that the two layer architecture is applied to the proposed architecture as opposed to keeping all the waveguides in one plane, thus avoiding significant crossing losses. To be specific, all the horizontal waveguides are placed in one layer while the vertical ones are placed in another layer. The inter-layer communication can be realized by the inter-layer couplers. MRs in these couplers can help the signal to make WN, WS, EN, and ES turns. M^2 MRs of the same size are partitioned into 4 groups and each group realizes one of the four turns, which can also be seen from Table I.

In order to allocate transmission resources in the switch fabric properly to each input-output communication, a horizontal (vertical) connection relationship, named as HCR (VCR), is set to connect these horizontal (vertical) waveguides in the switch fabric with the ones in the N input (output) ports.

By HCR, if we name the k th horizontal waveguide in the switch fabric as SH_k and the m th horizontal waveguide in the i th input port as $I_{i,m}$. $I_{i,m}$ should be connected to SH_k , when the following equation is satisfied:

$$k = (M/2) \times (i - M/2 \times \lfloor 2i/M \rfloor) + ((M/2)^2 - M/2) \times \lfloor 2m/M \rfloor + m. \quad (1)$$

By VCR, if we name the l th VWG in the switch fabric as SV_l and the n th VWG in the j th output port as $O_{j,n}$. $O_{j,n}$ should be connected to SV_l , when following equation is satisfied

$$l = (j - M/2 \times \lfloor 2j/M \rfloor) + (M/2) \times n. \quad (2)$$

Fig. 5 shows the architectures of the 2×2 (b), 4×4 (c), and 8×8 (d) SDM-based cells constructed according to the above introduction. Particularly, only one MR is needed in the 1×1 SBC, because there is one unique input-output pair, as shown in Fig. 5(a). In the 8×8 SBC, horizontal (vertical) waveguides in the switch fabric stay parallel and are sequentially numbered 0–31 from north (east) to south (west). The eight horizontal (vertical) waveguides in each input (output) port are sequentially numbered 0–7 from top (right) to bottom (left). In the HCR, according to the equation (1), the SH_{16} should be connected to the $I_{0,4}$, the SV_{12} should be connected to the $O_{4,3}$.

Although only one wavelength is employed in SBC of any size, it can provide non-blocking communication. Noticeably, two special kinds of communications are supported: i) it allows reuse of the same wavelength to realize two communications in the same waveguide at the same time. For instance, in Fig. 5(c), two input-output pairs, $I_2 \rightarrow O_2$ and $I_3 \rightarrow O_3$, can communication simultaneously in the same horizontal waveguide. ii) Any input port can transmit optical signals to M output ports simultaneously through M horizontal waveguides in the input port,

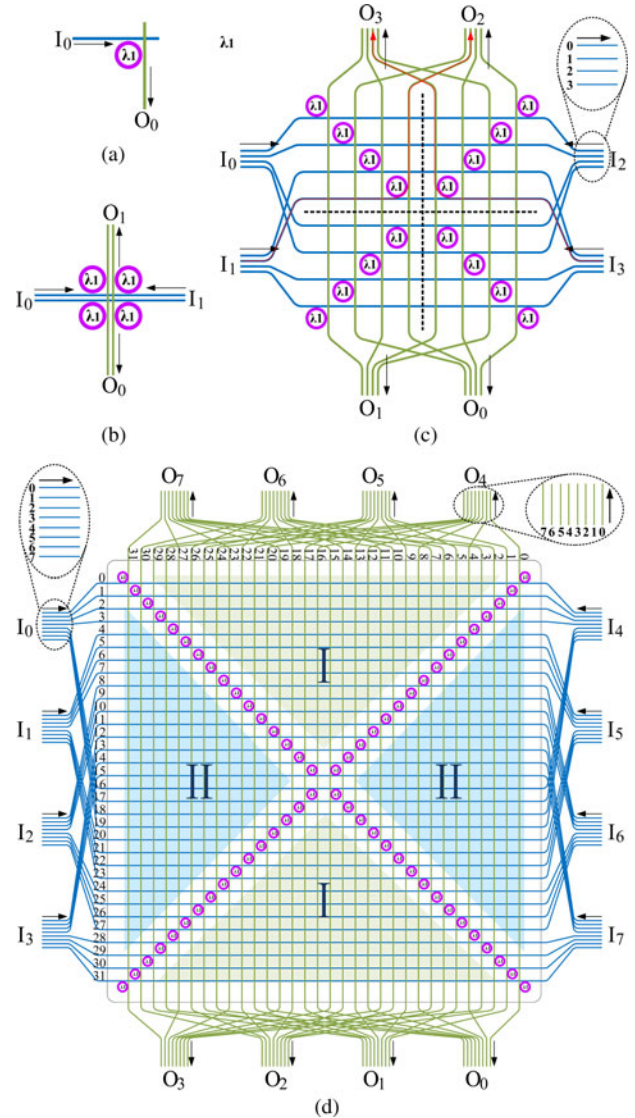


Fig. 5. The architecture of $M \times M$ SDM-based cell. (a) $M = 1$. (b) $M = 2$. (c) $M = 4$. (d) $M = 8$.

and vice versa. Thus, totally M^2 simultaneous communications can be supported, since each of the input-output pairs owns the exclusive waveguide communication channel.

The communication rules for the $M \times M$ (where $M = 2m$ and $m > 0$) SBC are made as follows. When the input port I_i communicates with the output port O_j , the optical signal will be injected into the $i_{((\lfloor 2i/M \rfloor + \lfloor 2j/M \rfloor) \% 2) \times ((j + M/2) \% M) + ((\lfloor 2i/M \rfloor + \lfloor 2j/M \rfloor + 1) \% 2) \times (M-1-j)}$ horizontal waveguide in I_i . For instance, in the 4×4 SBC, as shown in Fig. 5(c), optical signals from I_2 can reach O_0, O_1, O_2 , and O_3 by being injected into the 3rd, 2nd, 0th, and 1st horizontal waveguide in I_2 , respectively.

For the SBCs of the large sizes, the number of waveguides grows sharply with the value of M and has an adverse impact on area consumption. The number of waveguide crossings in HCR and VCR also increases exponentially and introduces more insertion loss for the signal. The utilization of waveguide resources drops sharply, since no optical signals will appear on

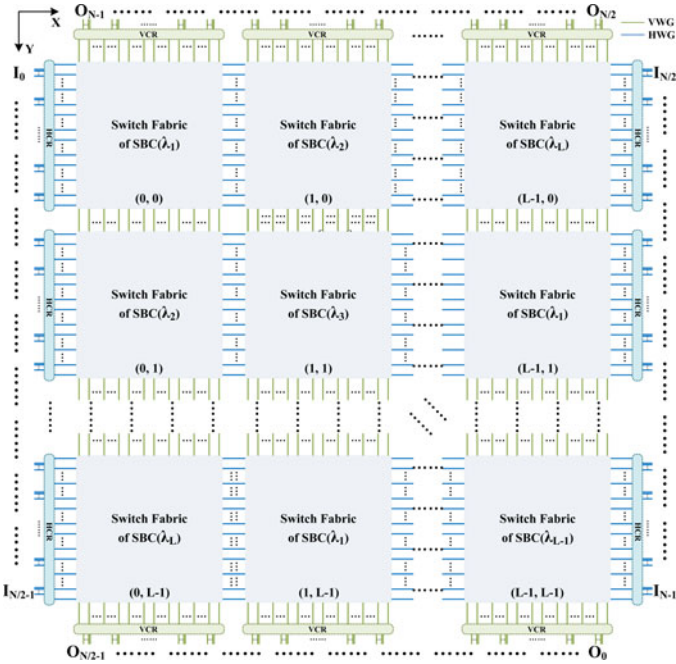


Fig. 6. The architecture of $N \times N$ POINT constructed by $M \times M$ SBCs.

the horizontal waveguides in region I and the VWGs in region II, as shown in Fig. 5(d). Therefore, we use small-size SBCs, such as 1×1 , 2×2 , 4×4 , and 8×8 , as the basic building block to provide different options for constructing $N \times N$ POINT in Section III.

III. ARCHITECTURE OF $N \times N$ POINT

The $M \times M$ (where $M = 1$ or $M = 2m$ and $m > 0$) SBC introduced in Section II is used as the basic building block to create $N \times N$ (where $N = 2n$ and $N \geq M$) POINT. Meanwhile, WDM is employed to improve the scalability of POINT. From Section II, all the MRs in an SBC have the same resonant wavelength, which is defined as the operating wavelength of the SBC. Different wavelengths represent different types of SBC. The SBC with the operating wavelength λ_i is named as $SBC(\lambda_i)$. The number of types of SBCs needed by the $N \times N$ POINT is L , which is determined by the equation (3) under the condition of the equation (4) constraint, in which the operator “%” means modulo operation

$$L = N/M \quad (3)$$

$$N \% M = 0. \quad (4)$$

Fig. 6 shows how $N \times N$ POINT is constructed by $M \times M$ (where $M = 2m$ and $m > 0$) SBCs. For each of L types of SBCs, it needs L copies. Totally L^2 SBCs are needed. The L^2 switch fabrics of these SBCs are connected in a mesh network. The neighboring switch fabrics are connected by $M^2/2$ waveguides. The position of a switch fabric is labeled as (x, y) . We assume the switch fabric in the northwest corner is labeled as $(0, 0)$. All the switch fabrics located on the left (top) and right (bottom) edges of the mesh network physically connects to the input (output) ports according to the HCR (VCR) of the $M \times M$ SBC.

In each row (column), the L switch fabrics logically share the M input (output) ports located on both sides. In other words, for the switch fabric (x, y) , together with the M input ports located on both sides of the y th row and the M output ports located on both sides of the x th column, logically forms a $M \times M$ SBC. In addition, the two layer architecture is still applied to the $N \times N$ POINT.

We propose a new wavelength assignment for the mesh network in order to realize the non-blocking communication. The mesh network adopts the XY routing algorithm, which means that optical signals from the input ports are always injected into the horizontal waveguides and ejected from the vertical ones and that each of these signals has to traverse a 90° turn in a SBC. In our wavelength assignment, each SBC is allocated a unique operating wavelength. To eliminate the contention in X-dimension and Y-dimension, all the SBCs in the same row or column have different operating wavelengths. Thus, each of L types of SBCs appears in each row or column only once. Optical signals with λ_i only turn in the switch fabric of $SBC(\lambda_i)$, passing by other SBCs in both X-dimension and Y-dimension. The operating wavelength λ_i assigned to the SBC containing switch fabric (x, y) can be calculated by

$$i = ((x + y) \% L) + 1. \quad (5)$$

Based on the wavelength assignment and the nonblocking SBC architecture, both inter- and intra- SBC communications are contention free. As a result, N^2 simultaneous communications can be supported. The communication rules for the constructed $N \times N$ POINT by $M \times M$ (where $M = 2m$ and $m > 0$) SBC are made as follows. When the input port I_i communicates with the output port O_j , the optical signals will turn in the switch fabric $(L - 1 - \lfloor 2j/M \rfloor \% L, \lfloor 2i/M \rfloor \% L)$ according to the rule of XY routing algorithm. The operating wavelength of the SBC containing switch fabric $(L - 1 - \lfloor 2j/M \rfloor \% L, \lfloor 2i/M \rfloor \% L)$ can be determined as $\lambda_{((x+y) \% L) + 1}$ according to the wavelength assignment, where x equals to $L - 1 - \lfloor 2j/M \rfloor \% L$ and y equals to $\lfloor 2i/M \rfloor \% L$. Consequently, $I_i \rightarrow O_j$ will communicate via the wavelength $\lambda_{((x+y) \% L) + 1}$. For instance, the turning point for $I_0 \rightarrow O_0$ is the switch fabric $(L - 1, 0)$ and this pair communicates via λ_L . After the wavelength is determined, optical signals should be injected into one of M waveguides in the input port properly by the communication rules for $M \times M$ SBC introduced in Section II.

As a special case, POINT ($M = 1$) is constructed by 1×1 SBC. The wavelength assignment and the communication rules for POINT ($M = 2m$ and $m > 0$) do not fit POINT ($M = 1$). For the 1×1 SBC, there is only one horizontal (vertical) waveguide in each input (output) port. Both HCR and VCR are one-to-one relationships. Therefore, different optical paths between the input ports and the output ports have to be established based on different wavelengths. Fig. 7(a) shows an example of 8×8 POINT ($M = 1$). It can be seen from the figure that all the 1×1 SBCs in the same row or column have different operating wavelengths and two identical 1×1 SBCs have to appear at the diagonal corners of spatial waveguide intersections, so that any communication can be realized without causing conflicts.

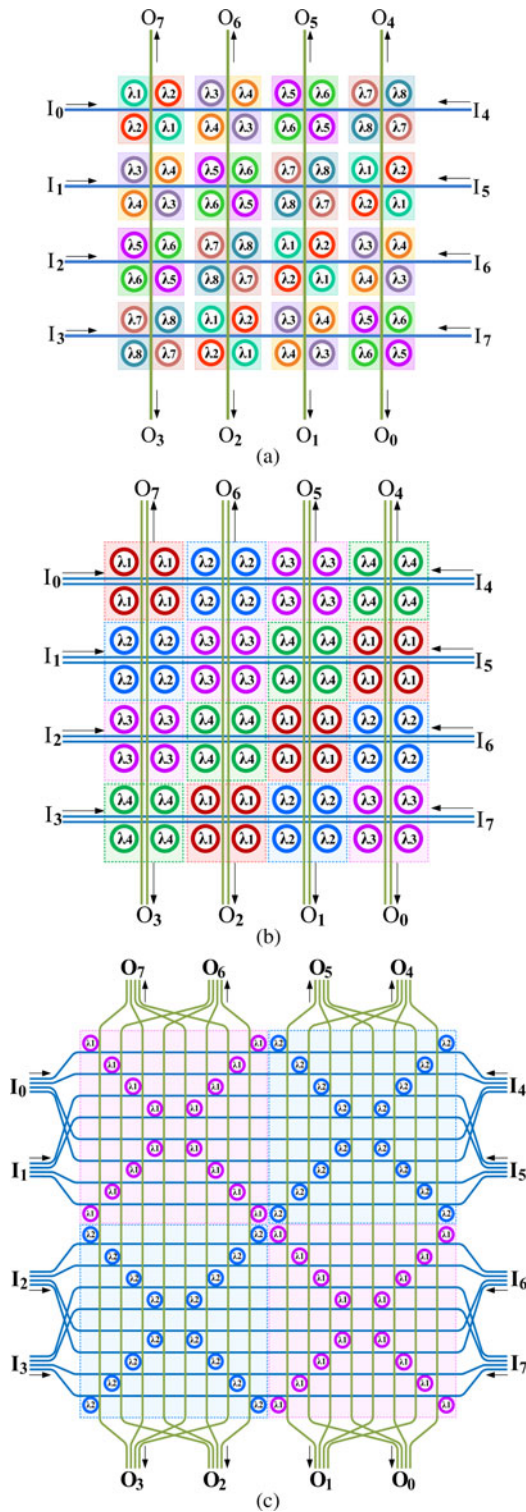


Fig. 7. The three architectures of 8×8 POINT. (a) $M = 1$. (b) $M = 2$. (c) $M = 4$.

Taking the 8×8 POINT as an example, M may be 1, 2, 4, or 8 according to equation (3) and (4). It means that an 8×8 POINT can be built by 1×1 , 2×2 , 4×4 , or 8×8 SBC and that an 8×8 POINT needs 8 types of 1×1 SBCs, 4 types of 2×2 SBCs, 2 types of 4×4 SBCs or one type of 8×8 SBC, respectively. We name these four different architectures of

TABLE II
NUMBER OF WAVELENGTHS USED IN DIFFERENT DESIGNS

	4×4	8×8	12×12	16×16	64×64
λ -router	4	8	12	16	64
GWOR	3	7	11	15	63
POINT($M=1$)	4	8	12	16	64
POINT($M=2$)	2	4	6	8	32
POINT($M=4$)	1	2	3	4	16
POINT($M=8$)	-	1	-	2	8

POINT as POINT ($M = 1$), POINT ($M = 2$), POINT ($M = 4$), and POINT ($M = 8$), respectively. Specially, $M = 8$ makes $L = 1$, thus, 8×8 POINT ($M = 8$) is built in exactly the same way as 8×8 SBC. By comparing three different 8×8 POINT architectures shown in Fig. 7, it is found that the 8×8 POINT ($M = 1$) uses the most number of wavelengths and has the most compact architecture. 8×8 POINT ($M = 4$) uses only two wavelengths, but introduces the highest area overhead. For 8×8 POINT ($M = 2$), it can make a tradeoff between the number of waveguides and area overhead. There is no waveguide crossing in 8×8 POINT ($M = 1$) and POINT ($M = 2$), but four waveguide crossings exist in each HCR or VCR of POINT ($M = 4$).

IV. COMPARISON AND DISCUSSION

In this section, we compare four representative POINTs with two existing typical passive OINs, the λ -router [12] and GWOR [13] from the following aspects including the number of wavelengths and MRs used, area overhead, and insertion loss.

Wavelength resources are precious in passive OIN design. There is an upper bound for the number of wavelengths that can be multiplexed in one waveguide [18], which will restrict the architecture scalability of passive OINs. From Table II, the number of wavelengths used in an $N \times N$ λ -router, GWOR, and POINT ($M = 1$) is N , $N - 1$, and N , respectively. In other words, the number of wavelengths in these three architectures increases linearly as the size of them increases. Consequently, their scalability is limited. It can also be seen from Table II that there is an inverse relationship between the number of wavelengths and the size of SBC, which is consistent with equation (3). The larger the size of SBC, the more times the same wavelength can be reused in different waveguides and the fewer the number of wavelengths will be needed in POINT. The following two cases will not happen. i) When N is 4 and M is 8, N is less than M . ii) When N is 12 and M is 8, the equation (4) is not true.

The number of MRs is a parameter in comparison and estimation of OIN designs, including not only the MRs used in OIN, but also the ones used in modulators before input ports and detectors after output ports. The numbers of MRs used in different designs are listed in Table III. To make a fair comparison, no self-communication is allowed (input signal from I_i will not go to O_i), since GWOR does not support self-communication. Thus, there exist $N(N - 1)$ possible input-output pairs in an $N \times N$ OIN. In POINT, all the $N(N - 1)$ input-output pairs have to employ $N(N - 1)$ MRs to realize non-blocking communication.

TABLE III
NUMBERS OF MRs USED IN DIFFERENT DESIGNS

	λ -router	GWOR	POINT ($M=1,2,4,8$)
8×8	160	160	168
16×16	704	704	720
64×64	12032	12032	12096
256×256	— (technically limited)	— (technically limited)	195840

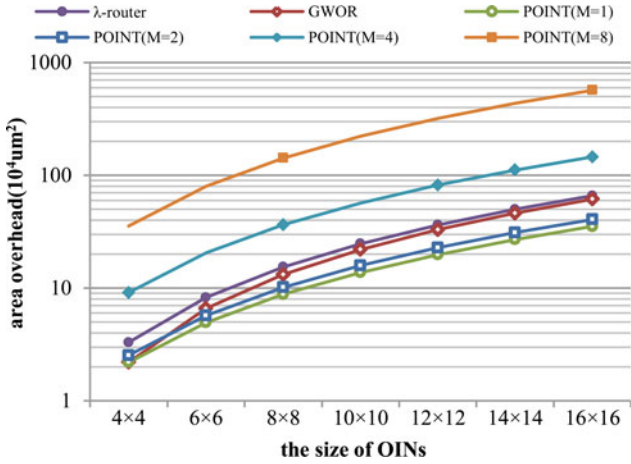


Fig. 8. The area of overhead in different passive networks.

However, in λ -router and GWOR, for directly connected input-output pair $I_i \rightarrow O_j$ ($i \neq j, i + j = N$), the input signal with the assigned wavelength will simply go straight to reach O_j , so that N MRs are saved. In addition, these three architectures employ the same number of MRs in modulators and detectors. For each input (output) port, a distinct input (output) wavelength is assigned for a different output (input) port. Therefore, $N - 1$ MRs are employed in each modulator (detector).

From Table III, the numbers of MRs used in the three designs are almost the same. POINT needs a few more MRs than λ -router and GWOR, which is trivial compared with the total number of MRs. POINT improves the scalability of itself significantly. For 256×256 OIN, POINT needs 195 840 MRs, which can be acceptable according to the study in [21], in which the proposed Corona, a typical high-bandwidth all-optical active OIN architecture, needs 1048 576 MRs. However, the scalability of λ -router or GWOR will be technically limited by the upper bound for the number of wavelengths that can be multiplexed in one waveguide [18].

To evaluate the area overhead introduced in these passive OINs, the related parameters given in [19] are adopted. The waveguide is 450 nm wide and all the MRs use the same waveguide dimension. The space between an MR and the waveguide is 200 nm. The separation space between two adjacent parallel waveguide is 5 μm . A square for a switching element introduces $74.16 \mu\text{m} \times 74.16 \mu\text{m}$ area overhead. The area overhead is presented in Fig. 8. It can be seen that the area for POINT ($M = 1$) is the smallest among all the passive OINs of any arbitrary size depending on its symmetrical and compact architecture. On the contrary, the curve of POINT ($M = 8$) grows sharply

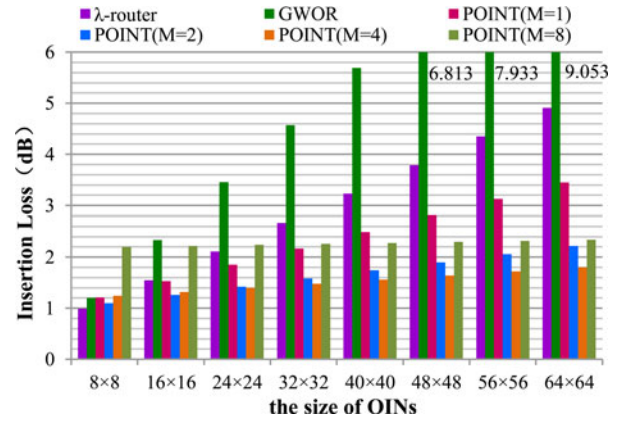


Fig. 9. The maximum insertion loss in different passive OINs.

with the size. It is estimated that the area for 64×64 POINT ($M = 8$) will reach 90.87 mm^2 , which introduces larger overhead. POINT ($M = 2$) require smaller area than GWOR and λ -router, because of the more compact architectures. Obviously, GWOR require a considerable area overhead because of its triangular architecture, as shown in Fig. 2(b).

Insertion loss determines not only the scalability and feasibility but also the power consumption for generating, modulating, and detecting the optical signals. The total insertion loss a packet experienced in the network is estimated by the following equation:

$$\begin{aligned} \text{Loss}(i, j) = & \text{IL}_{\text{drop}} + \sum \text{IL}_{\text{crossing}} + \sum \text{IL}_{\text{through}} \\ & + \sum \text{IL}_{\text{bending}} \end{aligned} \quad (6)$$

where IL_{drop} denotes the value of one drop-loss, which a signal only experiences once on its path in each of these passive OINs. Each MR in λ -router or GWOR has a drop-loss of 0.5 dB. According to [17], [18] and [20], inter-layer coupler introduces a 1 dB loss. $\sum \text{IL}_{\text{through}}$ denotes the total value of through-losses, and it is determined by the number of MRs the optical signal passed by, each MR has a through-loss of 0.01 dB. $\sum \text{IL}_{\text{crossing}}$ denotes the total value of waveguide crossing losses, each of which undergoes a 0.05 dB loss. $\sum \text{IL}_{\text{bending}}$ is the total value of waveguide bending losses, each of which is 0.013 dB. For fully connected passive networks, all valid optical paths are examined to determine the maximum and average network-level insertion loss IL_{max} and IL_{ave} . The maximum (average) insertion loss in different passive OINs of varying sizes is shown in Fig. 9 (see Fig. 10). Even though the IL_{max} of 4×4 GWOR is only 0.64dB, which is the lowest among all the 4×4 passive OINs. However, it can be seen from Fig. 9 that as the size of GWOR scales, IL_{max} increases significantly due to introducing more and more waveguide crossings. In POINT ($M = 1$) and POINT ($M = 2$), there is no waveguide crossing and bending because of the two layer architecture and the one-to-one relationships in their HCR and VCR. Consequently, the total insertion loss is substantially reduced.

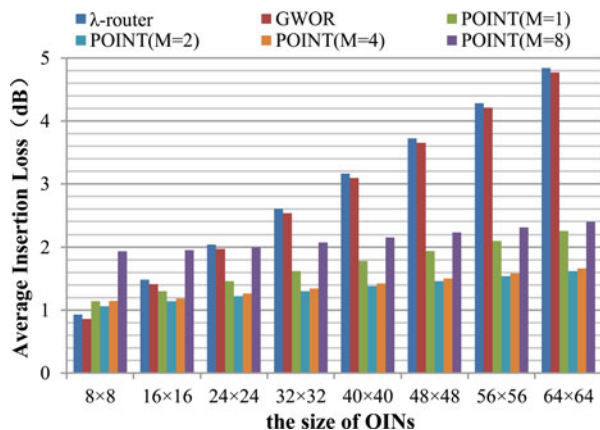


Fig. 10. The average insertion loss in different passive OINs.

V. CONCLUSION

In this paper, we propose a novel passive OIN, POINT, for ONoC architecture. POINT is a two-layer architecture, in which almost all the waveguide crossings are avoided. The $N \times N$ POINT is built by connecting $(N/M)^2 M \times M$ SBCs in a mesh network. The non-blocking communication within a SBC is realized by re-using only one wavelength on different communication channels. With the efficient wavelength assignment and communication rules, POINT can still provide non-blocking communication. Comparisons with existing passive OINs confirm that POINT can provide an optimal choice with the balance between the number of wavelengths, area overhead, and insertion loss for the same OIN size.

ACKNOWLEDGMENT

The authors would like to thank the editor and the anonymous reviewers for their insightful comments and suggestions, which improved the quality of the paper. The authors also want to thank H. Li, Z. Chen, L. Bai, and J. Zhang for many helpful discussions.

REFERENCES

- [1] D. Xiang and Y. Zhang, "Cost-effective power-aware core testing in NoCs based on a new unicast-based mul-ticast scheme," *IEEE Trans. Comput.-Aided Design*, vol. 30, no. 1, pp. 135–146, Jan. 2011.
- [2] R. Min, R. Ji, Q. Chen, L. Zhang, and L. Yang, "A universal method for constructing N-port nonblocking optical router for photonic networks on-chip," *J. Lightw. Technol.*, vol. 30, no. 23, pp. 3736–3741, 2012.
- [3] G. Chen, H. Chen, M. Haurylau, N. Nelson, D. Albonesi, P. Fauchet, and E. Friedman, "On-chip copper-based vs. optical interconnects: Delay uncertainty, latency, power, and bandwidth density comparative predictions," in *Proc. IEEE Int. Interconnect Technol. Conf.*, Jun. 2006, pp. 39–41.
- [4] K. Mo, Y. Ye, X. Wu, W. Zhang, W. Liu, and J. Xu, "A hierarchical hybrid optical-electronic network-on-chip," in *Proc. IEEE Comput. Soc. Annu. Symp. VLSI*, 2010, pp. 327–332.
- [5] C. Lea and B. Lin, "A new approach to the wavelength non-uniformity problem of silicon photon IC microrings," *J. Lightw. Technol.*, vol. 29, no. 17, pp. 2552–2559, 2011.
- [6] A. Biberman, B. Lee, N. Sherwood-Droz, M. Lipson, and K. Bergman, "Broadband operation of nanophotonic router for silicon photonic networks-on-chip," *IEEE Photon. Technol. Lett.*, vol. 22, no. 12, pp. 926–928, Jun. 2010.
- [7] Y. Xie, J. Xu, J. Zhang, Z. Wu, and G. Xia, "Crosstalk noise analysis and optimization in 5×5 hitless silicon-based optical router for optical networks-on-chip (ONoC)," *J. Lightw. Technol.*, vol. 30, no. 1, pp. 198–203, 2012.
- [8] A. Atef, I. O'Connor, and W. Heirman, "Performance evaluation for passive-type optical network-on-chip," in *Proc. IEEE Int. Symp. Rapid Syst. Prototyping*, Jun. 8–11, 2010, pp. 1–7.
- [9] A. Shacham, K. Bergman, and L. P. Carloni, "Photonic networks-on-chip for future generations of chip multiprocessors," *IEEE Trans. Comput.*, vol. 57, no. 9, pp. 1246–1260, Sep. 2008.
- [10] Z. Li, M. Mohamed, X. Chen, H. Zhou, A. Mickelson, L. Shang, and M. Vachharajani, "Iris: A hybrid nanophotonic network design for high-performance and low-power on-chip communication," *J. Emerging Technol. Comput. Syst.*, vol. 7, no. 2, p. 8, 2011.
- [11] H. Gu, K. Mo, J. Xu, and W. Zhang, "A low-power low-cost optical router for optical networks-on-chip in multiprocessor systems-on chip," in *Proc. Int. Symp. VLSI*, 2009, pp. 19–24.
- [12] M. Brière, B. Girodias, Y. Bouchebaba, G. Nicolescu, F. Gaffiot, and I. O'Connor, "System level assessment of an optical NoC in an MPSoC platform," in *Proc. Design, Autom. Test Eur. Conf. Exhib.*, Apr. 16–20, 2007, pp. 1–6.
- [13] X. Tan, M. Yang, L. Zhang, Y. Jiang, and J. Yang, "A generic optical router design for photonic network-on-chips," *IEEE J. Lightw. Technol.*, vol. 30, no. 3, pp. 368–376, Feb. 2012.
- [14] K. Preston, N. Sherwood-Droz, J. Levy, and M. Lipson, "Performance guidelines for WDM interconnects based on silicon microring resonators," in *Proc. Conf. Lasers Electro-Opt.*, May 2011, pp. 1–2.
- [15] C. Batten, A. Joshi, J. Orcutt, A. Khilo, B. Moss, C. Holzwarth, M. Popovic, H. Li, H. Smith, J. Hoyt, F. Kartner, R. Ram, V. Stojanovic, and K. Asanovic, "Building many-core processor-to-DRAM networks with monolithic CMOS silicon photonics," *IEEE Micro*, vol. 29, no. 4, pp. 8–21, Jul./Aug. 2009.
- [16] S. Beux, J. Trajkovic, I. O'Connor, G. Nicolescu, G. Bois, and P. Paulin, "Optical ring network-on-chip (ORNoC): Architecture and design methodology," in *Proc. Des., Autom. Test Eur. Conf. Exhib.*, Mar. 2011, pp. 1–6.
- [17] A. Biberman, N. Sherwood-Droz, X. Zhu, K. Preston, G. Hendry, J. Levy, J. Chan, H. Wang, M. Lipson, and K. Bergman, "Photonic network-on-chip architecture using 3D integration," *Proc. SPIE*, vol. 7942, p. 79420M-1, Feb. 2011.
- [18] X. Zhang and A. Louri, "A multilayer nanophotonic interconnection network for on-chip many-core communications," in *Proc. 47th Des. Autom. Conf.*, Jun. 13–18, 2010, pp. 156–161.
- [19] N. Sherwood-Droz, H. Wang, L. Chen, B. Lee, A. Biberman, K. Bergman, and M. Lipson, "Optical 4×4 hitless silicon router for optical networks-on-chip (NoC)," *Opt. Exp.*, vol. 16, no. 20, pp. 15915–15922, 2008.
- [20] R. Dokania and A. Apsel, "Analysis of challenges for on-chip optical interconnects," in *Proc. 19th ACM Great Lakes Symp. VLSI*, 2009, pp. 275–280.
- [21] D. Vantrease, R. Schreiber, M. Monchiero, M. McLaren, N. Jouppi, M. Fiorentino, A. Davis, N. Binkert, R. Beausoleil, and J. Ahn, "Corona: System implications of emerging nanophotonic technology," in *Proc. 35th Int. Symp. Comput. Archit.*, Jun. 21–25, 2008, pp. 153–164.

Authors' biographies not available at the time of publication.